

## Single-Crystal X-Ray and Powder Neutron Diffraction of ThB<sub>2</sub>C (ThB<sub>2</sub>C-Type)

PETER ROGL

*Institut für Physikalische Chemie, Universität Wien, A-1090 Wien, Währingerstrasse 42, Austria*

AND PETER FISCHER

*Labor für Neutronenstreuung, Eidgenössische Technische Hochschule Zürich, CH-5303 Würenlingen, Switzerland*

Received August 8, 1988; in revised form October 17, 1988

The crystal structure of ThB<sub>2</sub>C was determined using single-crystal X-ray and powder neutron diffraction data. ThB<sub>2</sub>C crystallizes in the rhombohedral space group  $R\bar{3}m$  with  $a = 0.66761(23)$ ,  $c = 1.13760(31)$  nm,  $c/a = 1.704$ ,  $V = 0.4391$  nm<sup>3</sup>,  $Z = 9$ . X-ray intensity data were obtained from a four-circle diffractometer; the structure was solved by Patterson methods and refined by full-matrix least-squares calculation.  $R = \Sigma|\Delta F|/\Sigma|F_o| = 0.034$  for an asymmetric set of 219 independent reflections ( $|F_o| > 2\sigma(F_o)$ ). Precise nonmetal atom parameters and bond distances have been derived from room-temperature neutron powder diffraction data employing the Rietveld–Young profile analysis method. The reliability value of the neutron refinement was  $R_1 = 0.067$ . The crystal structure of ThB<sub>2</sub>C is a new structure type with slightly puckered 6<sup>3</sup>-Th-metal layers alternating with nonmetal layers each composed of hexagons of boron atoms, the hexagons being linked by carbon atoms. Boron atoms are in a triangular prismatic metal surrounding of a tetrakaidekahedral coordination  $[\text{Th}_4\text{B}_2\text{C}_1]\text{B}$ , whereas carbon atoms occupy the center points of quadratic bipyramids  $[\text{Th}_4\text{B}_2]\text{C}$ . The crystal structure of ThB<sub>2</sub>C derives from the AlB<sub>2</sub>-type structure with carbon atoms entering the boron nets to form a  $\frac{2}{3} - (6\text{B}) \cdot (6\text{B}(3\text{C}))^2$  layer. © 1989 Academic Press, Inc.

### 1. Introduction

Early investigations (1, 2) of the thermodynamic phase equilibria in the actinoid–boron–carbon systems Th(U)–B–C reported on the formation of a variety of ternary compounds. Most of the phase equilibria and compounds were confirmed in the meantime and their crystal structures were established by X-ray single-crystal techniques (3–5). A recent reinvestigation of the uranium–boron–carbon system (6), however, revealed the existence of a hith-

erto unknown compound with the approximate formula UB<sub>2</sub>C and with a striking similarity of its X-ray powder pattern with the aforementioned ThB<sub>2</sub>C (1). In a preliminary structural chemical study (1), the ThB<sub>2</sub>C X-ray data were indexed on the basis of a simple hexagonal cell with  $a_0 = 0.3868$ ,  $c_0 = 0.3810$  at the carbon-rich phase boundary and  $a_0 = 0.3860$ ,  $c_0 = 0.3793$  at the carbon-poor end (1). The small hexagonal cell derived required a statistical occupation of B,C-atoms, therefore a superstructure ( $a_0$ ,  $3c_0$ ) introducing an ordered

B,C-kagomé net between the Th-layers was suggested by Toth *et al.* (1). Complete indexing (6) of the powder pattern of UB<sub>2</sub>C, however, disclosed an even larger (rhombohedral) cell ( $a_{\text{hex}} = a_0\sqrt{3}$ ,  $c_{\text{hex}} = 3c_0$ ) which also applied for the ThB<sub>2</sub>C phase. Based on this information a detailed study of the crystal structure of ThB<sub>2</sub>C became the subject of the present work.

## 2. Experimental

Two samples—one for X-ray diffraction and one containing the <sup>11</sup>B-isotope for the neutron experiments—each of a total amount of ca. 15 g were prepared by arc melting the elements together on a water-cooled copper hearth using a nonconsumable thoriated tungsten electrode in a Zr-gettered high-purity argon atmosphere. The starting materials were: thorium in the form of arc-melted buttons prepared from powder as obtained from Cerac Inc. with a claimed purity of 99.8%; carbon, reactor grade, impurities <1.4 ppm, Carbone Lorraine, France; boron, 98.15% <sup>11</sup>B-enriched isotope, AERE Harwell, UK, impurities <6000 ppm; and solid pieces of crystallized boron from H. C. Starck, Goslar, BRD, 99.8%.

To ensure homogeneity, the alloy buttons were turned over and remelted several times; weight losses were checked to be within 2% of the original weight. For annealing at 1600°C the alloys contained in cylindrical Knudsen-type carbon crucibles were heated for 48 hr in a tungsten sheet metal high-vacuum furnace at 10<sup>-4</sup> Pa. Starting from a nominal composition 25 at% Th, 50% B, and 25% C virtually single-phase and well-crystallized products were obtained in all cases. Only minor amounts of ThBC (less than about 10%) were observed for the <sup>11</sup>B-isotope containing alloy.

Precise lattice parameters and standard deviations were obtained by a least-squares refinement of room-temperature Guinier–

Huber X-ray powder data, using monochromatic CuK $\alpha_1$  radiation with an internal standard of 99.9999% pure Ge ( $a_{\text{Ge}} = 0.5657906$  nm). A small but significant variation was observed for the lattice parameters of the new compound confirming the existence of a small homogeneity region in agreement with earlier observations by (1).

### 2.1. Neutron Powder Diffraction

Neutron powder diffraction was performed at the Seibersdorf ASTRA-reactor, Austria, using the TKS-410 triple-axis spectrometer. Preferred orientation effects were minimized by powdering the sample to a grain size smaller than 30  $\mu\text{m}$ . Further details concerning the experiment are summarized in Table I. As indicated above, weak reflections of ThBC (see Ref. (3)) as a secondary phase were present for which a model profile was calculated according to the crystal data given in (3); the model profile was then subtracted from the sample profile employing a conversion factor for 8% of ThBC. The observed and corrected powder spectrum as used in the refinement is finally shown in Fig. 1.

Precise atom parameters, occupation numbers, individual thermal factors, and profile parameters were derived from a least-squares powder profile refinement procedure (7) including simultaneous refinement of the background (8). Neutron scattering lengths were taken from a recent compilation by Sears (9). A series of reliability measures was calculated, which are defined in detail in Table I.

### 2.2. Single-Crystal X-Ray Diffraction

A small single-crystal specimen suitable for X-ray diffraction was obtained by mechanical fragmentation of the arc-melted and annealed alloy. A first inspection of Weissenberg and precession photographs (axis [00.1]) revealed a hexagonal (rhombohedral) lattice geometry and the existence of a center of symmetry was displayed from

TABLE I  
EXPERIMENTAL DATA FOR ThB<sub>2</sub>C (NEUTRON POWDER DIFFRACTION)

Sample container	Vanadium cylinder, $R = 8$ mm
Temperature (K)	298 K
Radiation, wavelength (nm)	Neutrons, $\lambda = 0.120$ (1)
Absorption correction	—
Reactor	ASTRA, A-Seibersdorf
Monochromator	Zinc single crystal
$2\theta$ -Range ( $2\theta$ )	5.0 to 95.4
Step-scan increment ( $2\theta$ )	0.08
Coherent scattering lengths (fm)	Th 9.84 B[11] 6.65 C 6.65
Number of contributing reflections	201
Background	Background refinement (six parameters)
Preferred orientation	[001]
Number of variables	20
Largest element of correl. matrix	0.7
Maximal $\Delta/\sigma$	<0.01
<i>R</i> values:	
$R_I = \Sigma  I_i(\text{obs}) - (1/c)I_i(\text{calc})  / \Sigma I_i(\text{obs})$	
$R_F = \Sigma [ I_i(\text{obs}) ^{1/2} -  I_i(\text{calc}) ^{1/2}] / \Sigma [I_i(\text{obs})]^{1/2}$	
$R_P = \Sigma  Y_i(\text{obs}) - (1/c)Y_i(\text{calc})  / \Sigma Y_i(\text{obs})$	
$R_{WP} = [\Sigma w_i Y_i(\text{obs}) - (1/c)Y_i(\text{calc})]^2 / \Sigma w_i Y_i(\text{obs})^2]^{1/2}$	
$R_e = \{(N - P + C) / \Sigma w_i Y_i^2(\text{obs})\}^{1/2}$	
$\chi^2 = \{R_{WP} / R_e\}^2$	
$I_i$	Integrated intensity of reflection $i$
$w_i$	Weighting function
$Y_i$	Number of counts (background corrected) at $2\theta$
$c$	Scale factor

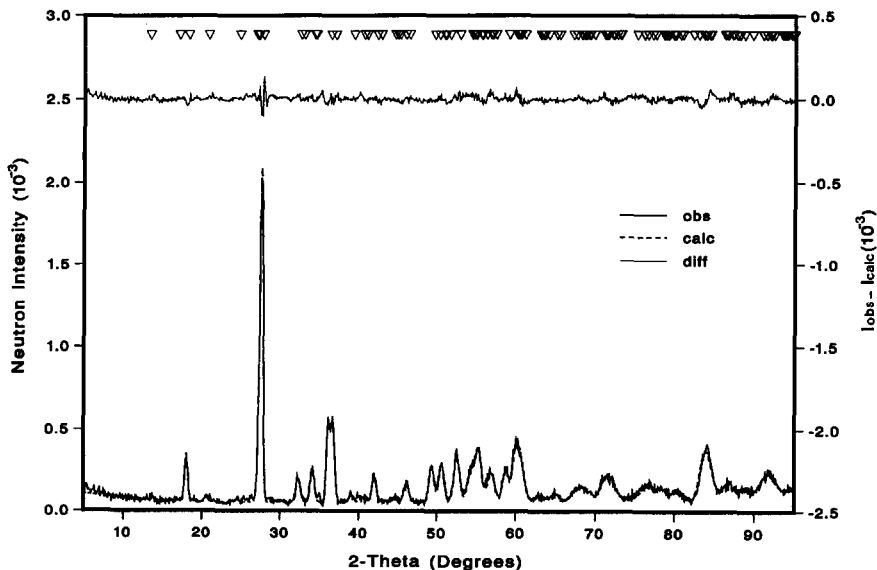


FIG. 1. Observed (solid line) and calculated (broken line) neutron powder diffraction profile of ThB<sub>2</sub>C (0.120 nm) at 298 K.

Integrated intensities were measured with graphite monochromatized  $\text{MoK}\alpha$  radiation on a STOE automatic four-circle diffractometer. A total of 1528 reflections were recorded up to a limit of  $\sin \theta/\lambda = 7.6$  nm. A set of 220 symmetry independent reflections was obtained by averaging "centered reflections" only, and all observed intensities (219 for  $|F_0| > 2\sigma$ ) were used in the refinement. An empirical absorption correction was applied using  $\psi$  (psi) scans of three independent reflections. Cell parameters were determined from a least-squares refinement of high angle  $2\theta$  values of 18 reflections. The crystallographic data are listed in Table II.

Space group,  $R\bar{3}m - D_{3d}^4$ , No. 166,  $Z = 9$ ; origin at center.  
The expression for the individual isotropic temperature factor is  $T = \exp[-B(\sin \theta/\lambda)^2] = \exp[-2\pi^2 U_{\text{iso}}(\sin \theta/\lambda)^2]$ .  
Anisotropic thermal factors are expressed as  $T = \exp[-2\pi^2(U_{11}h^2a^{*2} + U_{22}k^2b^{*2} + U_{33}l^2c^{*2} + 2U_{12}hka^*b^* + 2U_{13}hla^*c^* + 2U_{23}klb^*c^*) \cdot 10^{-2}]$ . By symmetry  $U_{11} = U_{22}$  and  $U_{13} = U_{23} = 0$ . The standard deviations are in parentheses.

Atom	Site	$x$	$y$	$z$	$B \text{ (nm}^2) \cdot 10^2$	$U_{11} (U_{\text{iso}})$	$U_{22}$	$U_{33}$	$U_{12}$
(A) Neutron powder diffraction at 298 K for Th <sup>11</sup> B <sub>2</sub> C									
Th(1)	3a	0	0	0	0.07( 7)				
Th(2)	6c	0	0	0.3142(4)	0.07( 7)				
C	9d	$\frac{1}{2}$	0	$\frac{1}{2}$	0.28(10)				
<sup>11</sup> B	18g	0.2767( 5)	0	$\frac{1}{2}$	0.59( 8)				
$a = 0.66761(23)$ , $c = 1.13760(31)$ nm, $c/a = 1.704$ , $V = 0.4391 \text{ nm}^3$ ; the calculated density is: $\rho_x = 9.054 \text{ Mg}^{-3}$ .									
Reliability factors: $R_1 = 0.067$ , $R_F = 0.046$ , $R_p = 0.095$ , $R_{\text{WP}} = 0.126$ , $R_e = 0.083$ , $\chi^2 = 2.30$ (for details see Table I).									
(B) X-ray single crystal data (sample melted and slowly cooled to RT)									
Th(1)	3a	0	0	0	0.84( 3)	0.84(3)	0.05(5)	0.42(2)	
Th(2)	6c	0	0	0.3156(1)	0.75( 3)	0.75(3)	0.05(4)	0.37(1)	
C	9d	$\frac{1}{2}$	0	$\frac{1}{2}$	0.74(26)	—	—	—	
B	18g	0.2762(18)	0	$\frac{1}{2}$	0.76(19)	—	—	—	
$a = 0.66995(41)$ , $c = 1.14467(48)$ nm, $c/a = 1.709$ , $V = 0.4450 \text{ nm}^3$ ; $\rho_x = 8.923 \text{ Mg}^{-3}$ , $\mu(\text{MoK}\alpha) = 71.8 \text{ mm}^{-1}$ .									
Correction for isotropic secondary extinction was $1.3(2) \times 10^{-6}$ .									
Reliability factors: $R_F = 0.034$ , $R_w = 0.030$ .									

### 3. Results and Discussion

#### 3.1. Structure Determination from X-Ray Single-Crystal Data

Nine formula units of  $\text{ThB}_2\text{C}$  were derived from a comparison of the atomic volumes with the volume of the unit cell assuming a space filling of 70%. The prominent peaks of a three-dimensional Patterson map  $P(u, v, w)$  were all found to be consistent with 3Th(1) in 3a and 6Th(2) in 6c ( $z \sim 0.31$ ) of the highest symmetrical space group  $R\bar{3}m$ . A difference Fourier map  $F_0 - F_{\text{Th}}$  clearly resolved the nonmetal atom sites: 9C in 9d and 18B in 18g. This structure model was refined using the STRUCSY full-matrix least-squares program system (STOE & Cie., Darmstadt, FRG). The weights used were based upon counting statistics  $w_i = 1/(\sigma(F_i))^2$ , and structure factors were furthermore corrected for isotropic secondary extinction; different weighting schemes were of no significant influence of the  $R$  value obtained. Refinement of the occupancies of the metal atoms did not result in a significant deviation from full occupation. The final  $R$  value calculated with anisotropic thermal parameters for the metal atoms was  $R = 0.034$  ( $R_w = 0.030$ ). At this point a difference map  $F_0 - F_c$  was featureless: The final positional

and thermal parameters are given in Table II; for interatomic distances see Section 3.2 and Table III. A listing of  $F_0$  and  $F_c$  values can be obtained on request.

#### 3.2. Neutron Powder Diffraction

Because of the small X-ray scattering power of the B,C-nonmetal atoms, precise information about the atom parameters and the occupational mode in  $\text{ThB}_2\text{C}$  were obtained from the neutron powder diffraction data. The final structural and profile parameters as well as the reliability values obtained from the least-squares refinement are presented in Table II, including simultaneous refinement of the background (8); atomic distances are shown in Table III. The occupancies of all atom sites have been refined; however, no significant deviation from a full occupation was revealed. As seen from Fig. 1 observed and calculated neutron diffraction intensities are in excellent agreement thereby confirming the atom arrangement as obtained from the X-ray single-crystal data refinement.

#### 3.3. Structural Chemistry

The crystal structure of  $\text{ThB}_2\text{C}$  (see Fig. 2) is a new representative of the nonmetal layer-type borocarbides as typical for a boron-to-metal ratio  $B/M \sim 2$  (for a classification of ternary metalborides and borocarbides see Ref. (10)). Slightly puckered 6<sup>3</sup>-layers of thorium atoms alternate with planar layers composed of regular hexagons of boron atoms with a bridging carbon atom between each two B-atoms of two neighboring B<sub>6</sub>-hexagons; the two-dimensional nonmetal layer is thus simply described as a planar  $6B \cdot (6B(3C))^2$ -net (for details see Fig. 1). Boron atoms occupy the center points of a triangular metal prism  $[\text{Th}_6\text{B}]$ ; with two additional boron and one carbon atoms an overall tetrakaidekahedral coordination figure is formed  $[\text{Th}_6\text{B}_2\text{C}]B$ . The carbon atoms are at the centers of a planar metal coordination  $[\text{Th}_4]C$ , com-

TABLE III  
INTERATOMIC DISTANCES FOR  $\text{ThB}_2\text{C}$   
(NEUTRON DIFFRACTION)

Th(1)– 6Th(2)	0.3861(1)	Th(2)–1Th(2)	0.4227(14)
– 2Th(2)	0.3574(7)	–3Th(2)	0.3879( 2)
–12B	0.3087(3)	–3Th(1)	0.3861( 1)
– 6C	0.2704(1)	–1Th(1)	0.3574( 7)
		–6B	0.2959( 5)
		–6B	0.2807( 6)
		–3C	0.2556( 5)
B– 2Th(1)	0.3087(3)	C–2Th(1)	0.2704( 1)
– 2Th(2)	0.2959(5)	–2Th(2)	0.2556( 5)
– 2Th(2)	0.2807(6)	–2B	0.1491( 5)
– 2B	0.1847(5)		
– 1C	0.1491(5)		

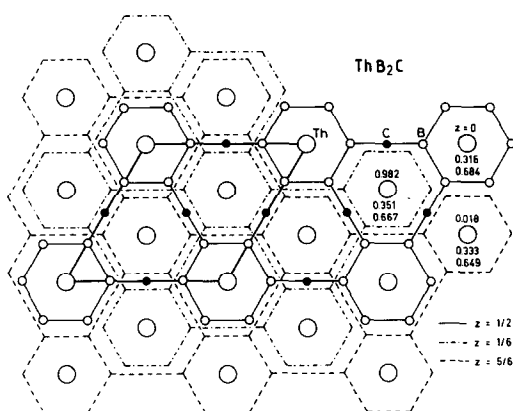


FIG. 2. The crystal structure of ThB<sub>2</sub>C as seen in a projection along [001]. The boron carbon nets and the heights of the Th atoms in the projection are outlined; the BC net in  $z = \frac{1}{2}$  is shown in detail.

pleted by two additional boron atoms at the vertices of a quadratic bipyramid [Th<sub>4</sub>B<sub>2</sub>]C. There are no direct carbon-carbon contacts in the structure. The formal substitution of a boron atom in the octahedral metal-carbon coordination [T<sub>6</sub>]C as typical for most transition metal carbides was earlier observed in the monoborocarbides of the actinoid elements where a [An<sub>3</sub>B]C-bipyramid is formed (3–5). Carbon-thorium bond distances (average 0.2630 nm; see Table III) are close to the sum of radii and correspond to the average distances in ThBC (0.2639 nm) and in Th<sub>3</sub>B<sub>2</sub>C<sub>3</sub> (0.2627 nm for the C2 atoms). With an increasing number of bonds formed to boron atoms at the expense of carbon-metal bonds, the carbon-boron bond lengths tend to decrease: 0.1553 nm in Th<sub>3</sub>B<sub>2</sub>C<sub>3</sub>, 0.1541 nm in ThBC, and 0.1491 nm in ThB<sub>2</sub>C.

The boron hexagons are centered above and below by thorium atoms in close resemblance to the AlB<sub>2</sub>-type of structure and the boron-boron bond lengths of 0.1847 nm are in good agreement with B-B distances in the AlB<sub>2</sub>-type diborides of the larger rare-earth metals; i.e., B-B = 0.1916 nm for the

high-temperature compound GdB<sub>2</sub>. The similar alloying behavior of thorium and of the larger RE metals (Nd, Sm) in ternary boride phases has been mentioned earlier (10) and is partly based on a comparable atom size. With increasing ratio  $R_M/R_{RE}$  the stability of AlB<sub>2</sub>-type phases is decreasing and SmB<sub>2</sub> is only obtained from high-pressure synthesis at elevated temperature; no ThB<sub>2</sub> is formed in thermodynamic equilibrium. The crystal structure of ThB<sub>2</sub>C can thus be seen as a stabilization of an AlB<sub>2</sub>-type derivative by carbon modifying the boron nets to adapt for the larger thorium atoms.

Boron-carbon net-type borocarbides are well known from the structure types of rare-earth compounds such as: ScB<sub>2</sub>C<sub>2</sub> (11), LaB<sub>2</sub>C<sub>2</sub> (12), and YB<sub>2</sub>C (13). Whereas the structure type of ThB<sub>2</sub>C is found with all the light actinoid metals Th, U (6) and Pu (14), CeB<sub>2</sub>C (15) so far has been the only isostructural rare-earth compound—the borocarbides of the smaller rare-earth members (Sc, Y, Gd → Lu)B<sub>2</sub>C adopt the YB<sub>2</sub>C-type which directly derives from binary UB<sub>4</sub> (YB<sub>2</sub>C□).

Depending on the boron and carbon content of samples near ThB<sub>2</sub>C, a significant variation of the unit cell dimensions was observed, whereby the lower volume corresponded with the boron-poor phase boundary. Because of the generally larger size of the boron atoms with respect to carbon atoms ( $R_B/R_C \sim 1.14$ ) boron/carbon substitution is therefore inferred at off-stoichiometric concentrations Th(B<sub>1-x</sub>C<sub>x</sub>)<sub>2</sub>C, with carbon atoms now entering the B<sub>6</sub>-hexagons.

Although carbon-net formation is rarely observed in transition-metal carbides, there is a significant tendency for carbon atoms to substitute for boron in typical boron aggregations such as, i.e., in the  $\frac{2}{3}$  boron networks of EuB<sub>6-x</sub>C<sub>x</sub> (B<sub>6</sub>-octahedra) (16, 17)) and in the  $\frac{2}{3}$  boron nets of ErB<sub>2-x</sub>C<sub>x</sub> (B<sub>6</sub>-hexagons, AlB<sub>2</sub>-type (18)).

### 3.4. Melting Point Data, Magnetism, and Superconductivity of ThB<sub>2</sub>C

The melting temperature of ThB<sub>2</sub>C was measured in a crucible-free Pirani furnace; design details of the apparatus used, of sample form required, and of calibration procedures applied were described earlier (19). Three samples with a total weight of ca. 5 g each were prepared as powder compacts from the prereacted single-phase material used for the X-ray single-crystal study. The bar-shaped specimens were first degassed at lower temperatures in vacuum and subsequently preequilibrated at sub-solidus temperatures under  $1.2 \times 10^5$  Pa of high-purity argon. Calibration was made against an electron beam melted rod of 99.99% van-Arkel hafnium with a measured melting point of  $2228 \pm 12^\circ\text{C}$ . Accordingly the melting point of congruently melting ThB<sub>2</sub>C as determined from three independent measurements was  $2040 \pm 15^\circ\text{C}$ .

Magnetic susceptibilities measured in the range from 1.5 to 1100 K revealed ThB<sub>2</sub>C to be weakly paramagnetic (20), and no superconductivity has been observed down to 1.5 K.

### Acknowledgments

This research was supported by the Austrian Science Foundation (Fonds zur Förderung der wissenschaftlichen Forschung in Österreich) under Contract P5523. Thanks are due to Dr. B. Krismer, from H. C. Starck GmbH, Goslar, BRD, for the kind supply of boron powder. The neutron powder experiments were carried out at the Seibersdorf-Astra reactor; we kindly thank Dr. B. Kunsch and J. Rupp for the neutron powder diffraction data collection. P.R. is grateful to the Austrian Ministry for Science and Research for grant-

ing a scholarship for the neutron diffraction data refinement in Würenlingen, Schweiz.

### References

1. L. E. TOTH, F. BENESOVSKY, H. NOWOTNY, AND E. RUDY, *Monatsh. Chem.* **92**, 956 (1961).
2. L. E. TOTH, H. NOWOTNY, F. BENESOVSKY, AND E. RUDY, *Monatsh. Chem.* **92**, 794 (1961).
3. P. ROGL, *J. Nucl. Mater.* **73**, 198 (1978).
4. P. ROGL, *J. Nucl. Mater.* **79**, 154 (1979).
5. P. ROGL, *J. Nucl. Mater.* **80**, 187 (1979).
6. P. ROGL, J. BAUER, AND J. DEBUIGNE, *J. Nucl. Mater.*, in press.
7. H. M. RIETVELD, *J. Appl. Crystallogr.* **2**, 65 (1969).
8. D. B. WILES AND R. A. YOUNG, *J. Appl. Crystallogr.* **14**, 149 (1981).
9. V. F. SEARS, Chalk River Nuclear Laboratories, Report AECL-8490 (1984).
10. P. ROGL, *J. Less-Common Met.* **110**, 283 (1985).
11. G. S. SMITH, Q. JOHNSON, AND P. C. NORDINE, *Acta Crystallogr.* **19**, 668 (1965).
12. J. BAUER AND O. BARS, *Acta Crystallogr. Sect. B* **36**, 1540 (1980).
13. J. BAUER, *J. Less-Common Met.* **87**, 45 (1982).
14. P. ROGL, P. E. POTTER, AND H. R. HAINES, to be published.
15. F. BONHOMME, P. GOSSELIN, D. ANSEL, AND J. BAUER, "Etude Crystallochimique du Systeme Cerium-Bore-Carbone," Projet de fin d'études 5 èm G. P. INSA, Rennes, Juin (1988).
16. K. A. SCHWETZ, M. HOERLE, AND J. BAUER, *Ceramurgia Int.* **5**(3), 105 (1979).
17. J. M. TARASCON, J. L. SOUBEYROUX, J. ETOURNEAU, R. GEORGES, J. M. D. COEY, AND O. MASENET, *Solid State Commun.* **37**, 133 (1981).
18. F. CHAPIUS, T. JOSSIC, AND J. BAUER, "Etude de la Solubilité du Carbone dans le Diborure d'Erbium," Projet de fin d'études 5 èm G. P., INSA, Rennes, Juin (1977).
19. E. RUDY, S. WINDISCH, AND Y. A. CHANG, Air Force Materials Laboratory Technical Report, Wright-Patterson Air Force Base, Ohio, AFML-TR-65-2, Part I, Vol. I, (1965).
20. B. RUPP, P. ROGL, AND I. FELNER, *J. Nucl. Mater.*, in press.